Electronic Supplementary Material (ESI) for Sustainable Energy & Fuels.

High-energy hybrid lithium-ion capacitor enabled by a mixed capacitive - battery storage $LiFePO_4$ – AC cathode and a SnP_2O_7 – rGO anode

Miguel Granados-Moreno[a], Gelines Moreno-Fernández[*,a], Roman Mysyk[a], Daniel Carriazo[*,a,c]

[a] Centre for Cooperative Research on Alternative Energies (CIC energiGUNE), Basque Research and Technology Alliance (BRTA), Alava Technology Park, Albert Einstein 48, 01510 Vitoria-Gasteiz, Spain.

[b] Universidad del País Vasco, UPV/EHU, 48080 Bilbao, Spain

[c] IKERBASQUE, Basque Foundation for Science, 48013 Bilbao, Spain

[*]Corresponding authors, Tel: +34 94 529 71 08; E-mail: mamoreno@cicenergigune.com and dcarriazo@cicenergigune.com

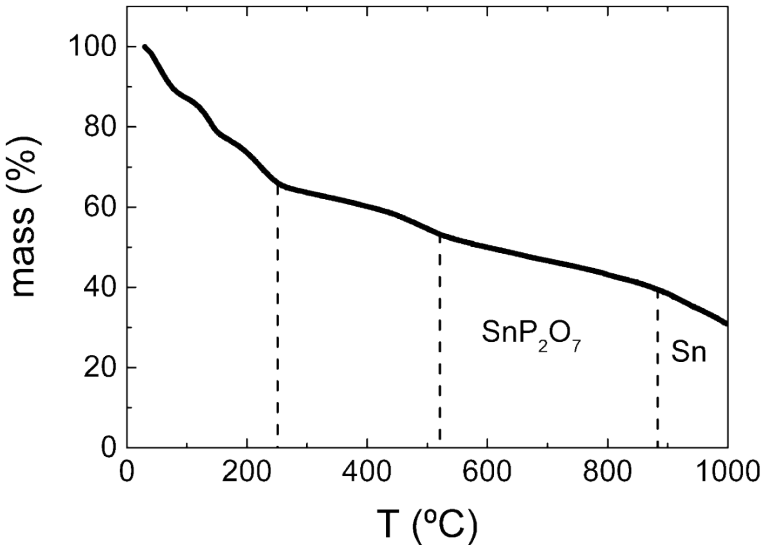

Fig. S1 TGA curve registered under Ar atmosphere for the precursor of the negative electrode materials

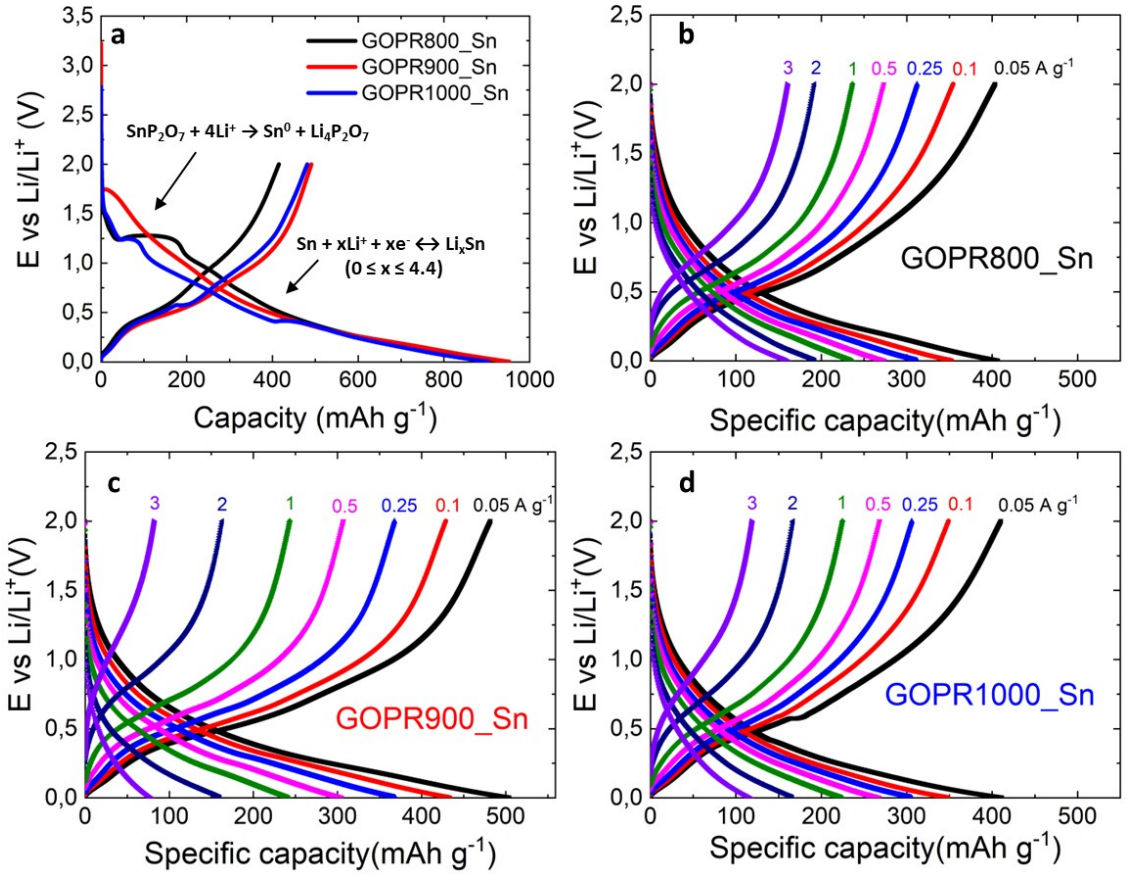

Fig. S2 Comparison of the first cycle recorded at 0.05 A g^{-1} for the three materials (a), galvanostatic charge/ discharge profiles at different current densities for GOPR800_Sn (b), GOPR900_Sn (c) and GOPR1000_Sn (d)

In Figure S3 are shown the SEM images of Sn-based composites before and after cycling. It can be observed that nanosized crystalline SnP_2O_7 particles are transformed into a $Li_4P_2O_7$ matrix and nano Sn (0) particles. Due to the small size of the Sn (0) particles and because they are embedded into the $Li_4P_2O_7$ matrix, it is challenging to directly observe them. Despite that, it is possible to identify those particles by using the BSED detector of the SEM. Fig S3a and S3b show the SEM images of the pristine GOPR800-Sn obtained using the ETD detector, where the SnP_2O_7 particles are easily identified while Fig S3c and S3d show the SEM images of the cycled GOPR800-Sn obtained by ETD and BSED detectors respectively, where we can observe the SEI and the $Li_4P_2O_7$ matrix covering the reduced graphene oxide sheets, and the Sn (0) particles embedded in it.

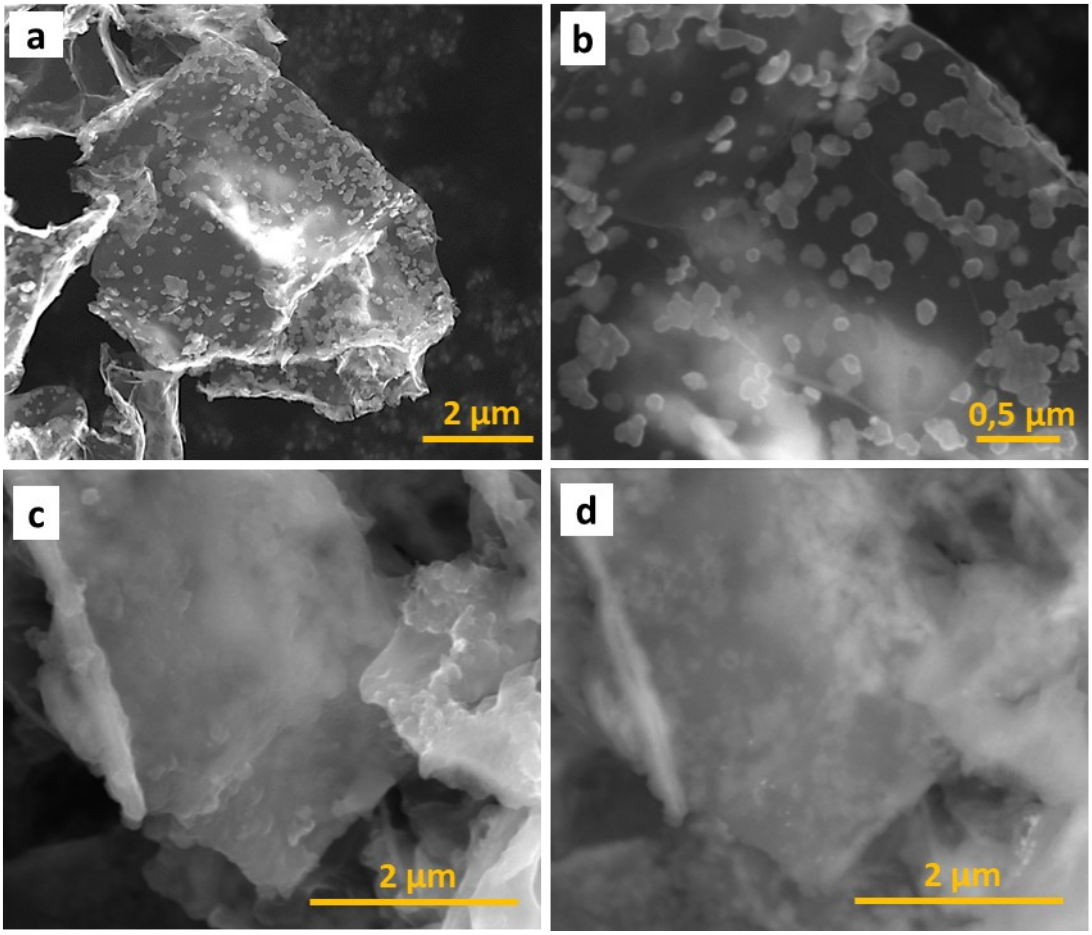

Fig. S3 SEM images of: as-synthesized GOPR800_Sn (a, b), GOPR800_Sn material after cycling (c) using ETD detector and GOPR800_Sn after cycling test observed by BSED detector (d).

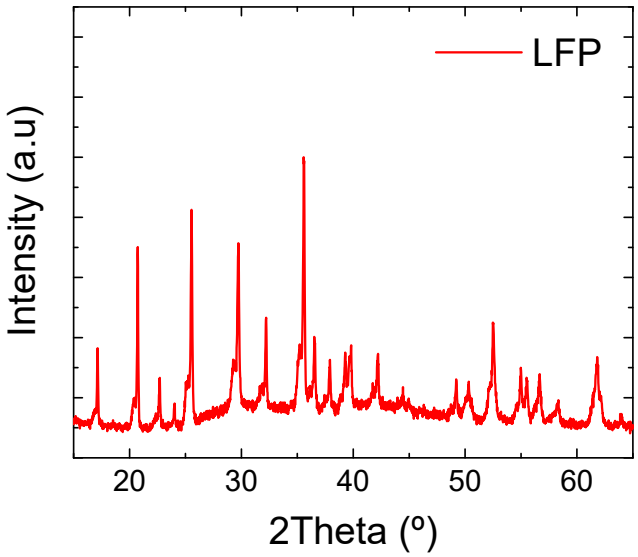

Fig. S4 XRD of synthetized lithium iron phosphate (LFP)

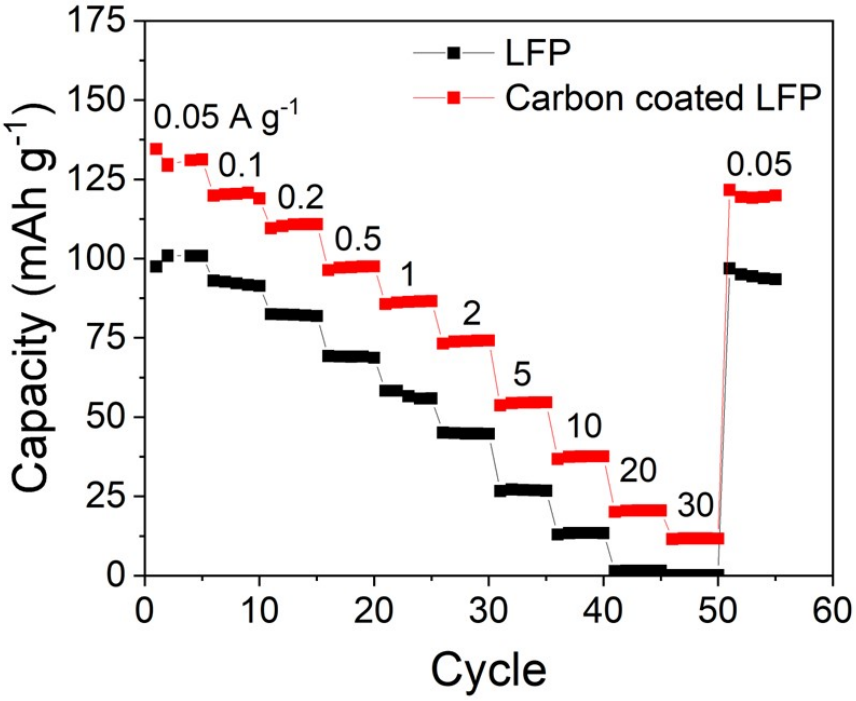

Fig. S5 Rate capability of LFP and carbon coated LFP.

Post cycling analysis performed on the LFP-based electrodes in half cell configuration are included in Figure S6. As depicted in in this figure, the size and shape of LFP agglomerates before (Fig 6a and Fig 6b) and after (Fig 6c and Fig 6d) cycling is similar. The nanometric size of LFP particles is supposed to prevent cracks on the LFP surface and maintain the particle size and morphology.

With respect to the crystallinity of LFP particles, Fig 6e shows the XRD spectrum of the RG-LFP powder after the cycling test. Although the residual peaks can be ascribed to LFP, most characteristic peaks for LFP are not discerned whereas the low intensity of the present diffraction peaks points out that a major part of LFP particles becomes amorphous upon cycling. The amorphization of LFP particles caused by the nanometric size of the particles and the contact with the outer carbon layer is underlined in the manuscript.

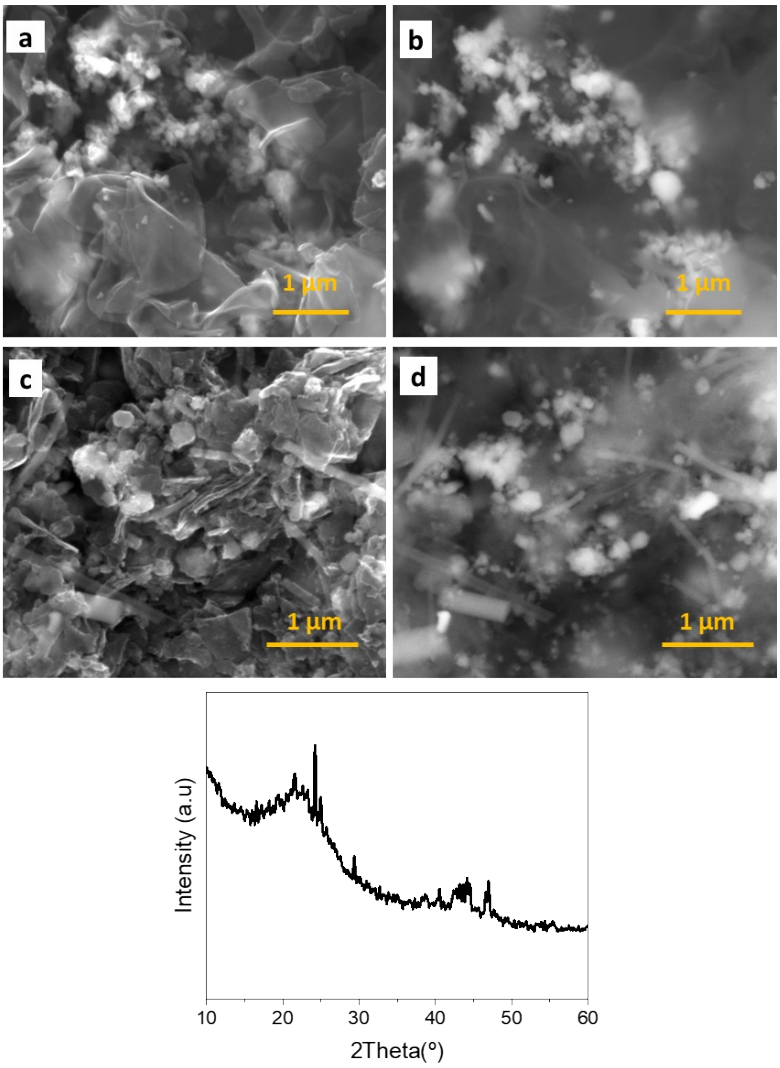

Fig. S6 SEM images of RG-LFP composite before (a and b) and after cycling test (c and d), observed by ETD and BSED detectors, respectively. (e) XRD diffraction pattern of RG-LFP electrode after cycling test.

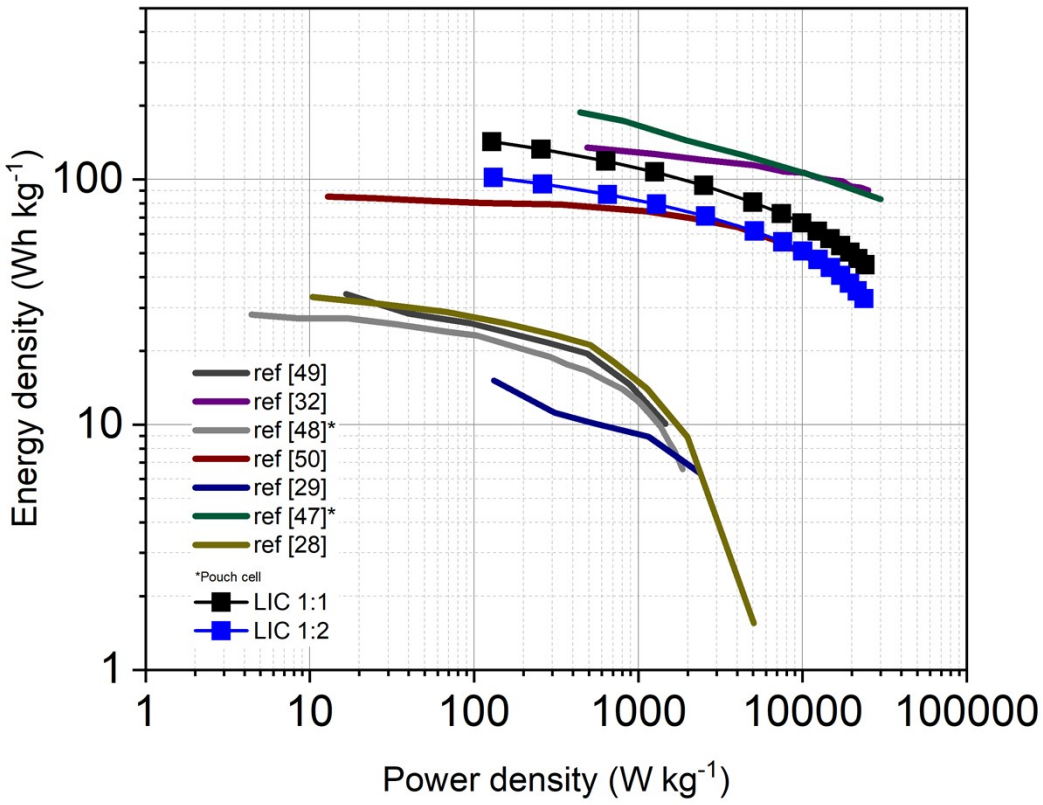

Fig. S7 Ragone plot, including the energy and power density values achieved in our LICs and some representative results reported in literature.